Clinically Relevant Effects of Convection-Enhanced Delivery of AAV2-GDNF on the Dopaminergic Nigrostriatal Pathway in Aged Rhesus Monkeys

Louisa C. Johnston,[1] Jamie Eberling,[2] Philip Pivirotto,[1] Piotr Hadaczek,[1] Howard J. Federoff,[3] John Forsayeth,[1] and Krystof S. Bankiewicz[1]

Abstract

Growth factor therapy for Parkinson's disease offers the prospect of restoration of dopaminergic innervation and/or prevention of neurodegeneration. Safety and efficacy of an adeno-associated virus (AAV2) encoding human glial cell-derived neurotrophic factor (GDNF) was investigated in aged nonhuman primates. Positron emission tomography with 6-[^{18}F]-fluoro-L-m-tyrosine (FMT-PET) in putamen was assessed 3 months before and after AAV2 infusion. In the right putamen, monkeys received either phosphate-buffered saline or low-dose (LD) or high-dose (HD) AAV2-GDNF. Monkeys that had received putaminal phosphate-buffered saline (PBS) infusions additionally received either PBS or HD AAV2-GDNF in the right substantia nigra (SN). The convection-enhanced delivery method used for infusion of AAV2-GDNF vector resulted in robust volume of GDNF distribution within the putamen. AAV2-GDNF increased FMT-PET uptake in the ipsilateral putamen as well as enhancing locomotor activity. Within the putamen and caudate, the HD gene transfer mediated intense GDNF fiber and extracellular immunoreactivity (IR). Retrograde and anterograde transport of GDNF to other brain regions was observed. AAV2-GDNF did not significantly affect dopamine in the ipsilateral putamen or caudate, but increased dopamine turnover in HD groups. HD putamen treatment increased the density of dopaminergic terminals in these regions. HD treatments, irrespective of the site of infusion, increased the number of nonpigmented TH-IR neurons in the SN. AAV2-GDNF gene transfer does not appear to elicit adverse effects, delivers therapeutic levels of GDNF within target brain areas, and enhances utilization of striatal dopamine and dopaminergic nigrostriatal innervation.

Introduction

THE INCIDENCE AND PREVALENCE of Parkinson's disease (PD) increase dramatically for individuals over the age of 50 years (Tanner and Goldman, 1996). The pathogenesis of PD, therefore, occurs in the setting of normal age-related functional changes in the brain. PD involves progressive degeneration of dopaminergic neurons of the substantia nigra pars compacta (SNc) in the midbrain, which project to the motor striatum via the nigrostriatal pathway. Clinical symptoms emerge when at least 60% of these neurons are lost (Nyholm, 2007). At clinical presentation of motor symptoms, striatal dopamine (DA) has decreased by at least 80% of the normal level typically found in this region of the forebrain (Berheimer et al., 1973; Kish et al., 1992). Various other path-

ological changes occur during the course of this disease (Braak and Braak, 2000), but the nigrostriatal insult represents the core determinant of the principal motor features of PD that include akinesia, rigidity, and tremor.

Neurotrophic factors can promote the survival and maintenance of neurons in the central nervous system (Airaksinen and Saarma, 2002). One of the most potent trophic factors for nigral dopaminergic neurons is glial cell-derived neurotrophic factor (GDNF). Some PD patients have experienced significant clinical benefit after putaminal infusions of GDNF (Gill et al., 2003; Patel et al., 2005; Slevin et al., 2005, 2006). Controversial clinical results have led to the current opinion that, before recombinant GDNF can be pursued further as a therapy for PD, a better delivery protocol and dosing regimen must be established (Sherer et al., 2006). As GDNF protein

[1]Department of Neurological Surgery, University of California San Francisco, San Francisco, CA 94103.
[2]Department of Molecular Imaging and Neuroscience, Lawrence Berkeley National Laboratory, Berkeley, CA 94720.
[3]Georgetown University Medical Center, Washington, DC 20007.

delivery must occur over long periods of time, it probably will require an indwelling cannula coupled to a minipump system. The use of gene therapy for the delivery of GDNF to the nigrostriatal system provides an alternative means by which constitutive or regulated GDNF production can be achieved. However, the clinical success of this approach is similarly dependent on an optimal delivery protocol, dosing regimen, and overall study design.

Both adenoviral (Kozlowski *et al.*, 2001) and lentiviral GDNF vectors have been evaluated preclinically in aged or parkinsonian monkeys (Kordower *et al.*, 2000; Palfi *et al.*, 2002). However, such platforms represent less than ideal strategies for safe use in humans. For example, DNA is randomly inserted by the lentivirus into the host genome in contrast to adeno-associated viral (AAV) vectors, which are maintained primarily as episomal concatemers (Yang *et al.*, 1999). Use of adenoviral vectors has been confounded by cytotoxicity issues (Lowenstein and Castro, 2003). Our work and that of others has demonstrated that AAV type 2 (AAV2) can be delivered by convection-enhanced delivery (CED) over a wide dose range without harmful effects on the brain, most importantly in humans (for a perspective, see Fiandaca *et al.*, 2008). As such, AAV2 represents a safer option for transduction of neurons in the brain (Kanter-Schlifke *et al.*, 2007).

Aging nonhuman primates display changes in nigrostriatal function, characterized by both mild striatal DA deficit and appearance of motor deficits, as well as accumulation of potentially neuroinflammatory by-products of DA synthesis in nigral neurons (Emborg *et al.*, 1998; McCormack *et al.*, 2004). Putaminal GDNF infusions have been shown to increase dopaminergic tone in the striatum as well as improve the impaired motor function normally observed in aged monkeys (Maswood *et al.*, 2002). A lentiviral GDNF vector system increased dopaminergic innervation of the striatum of aged rhesus macaques (Kordower *et al.*, 2000). The study by Kordower and colleagues employed a magnetic resonance imaging (MRI)-assisted microinjection method for vector delivery that is prone to reflux. Our laboratory has pioneered the use of CED of AAV (Bankiewicz *et al.*, 2000; Hadaczek *et al.*, 2006a). This results in bulk flow of vector particles away from the tip and into the surrounding parenchyma (Hadaczek *et al.*, 2006b), resulting in broad distribution of vector throughout the targeted region. To date, the long-term safety and effects of AAV2 carrying a cDNA for human GDNF has not been evaluated in aged monkeys.

The aim of this investigation was to determine whether the CED-based volume of infusate planned for the human clinical trial of AAV2-GDNF is well tolerated in aged rhesus macaques, because AAV2-GDNF is envisaged for use in older patients. As such, this study may be regarded as a definitive safety nonclinical study because it intentionally doses aged animals with levels of GDNF in excess of what we would envisage in the clinic. A companion 2-year efficacy study in 1-methyl-4-phenyl-1,2,3,6-tetrahydropyridine (MPTP)-lesioned monkeys is currently underway. Our characterization of the effects of this vector in aged nonhuman primates on the nigrostriatal system through positron emission tomography (PET) imaging, behavioral, neurochemical, immunohistochemical, and biochemical assessments has helped to define more clearly the relationship between vector dose and safety-related aspects of vector dose and anatomic location.

Materials and Methods

Animals

These experiments were performed on 14 naive male and female rhesus macaques (more than 20 years old), in accordance with guidelines of the University of San Francisco California (San Francisco, CA). The animals were housed separately in home cages in a temperature-controlled room and exposed to a 12-hr light/dark cycle. They were fed twice daily with amounts appropriate for the size and age of the animals, and water was freely available. Diet was supplemented with fruit or vegetables daily. Experimentation was performed according to the National Institutes of Health guidelines and to the protocols approved by the Institutional Animal Care and Use Committee at the University of California San Francisco. Clinical evaluations and *in vivo* imaging by MRI and PET was performed before gene transfer. At the completion of the study, animals were killed, and then tissue was analyzed by histochemical and biochemical methods.

AAV2-GDNF vector construction

The human GDNF cDNA was cloned into an AAV2 shuttle plasmid, and a recombinant AAV2 carrying GDNF under the control of the cytomegalovirus promoter was generated by a triple transfection technique and subsequent purification by CsCl gradient centrifugation (Matsushita *et al.*, 1998; Wright *et al.*, 2003). AAV2-GDNF was concentrated to 1.1×10^{13} vector genomes per milliliter (vg/ml) as determined by quantitative polymerase chain reaction (PCR).

Magnetic resonance imaging

Baseline MRIs were performed to enable accurate placement of the infusion cannula in the target structures and to align with histological images for estimation of the volume of distribution. During the MRI procedure monkeys were sedated with ketamine (Ketaset, 7 mg/kg, intramuscular) and xylazine (Rompun, 3 mg/kg, intramuscular). Each animal was positioned in the MRI-compatible stereotactic frame. Ear- and eye-bar positions were recorded, and an intravenous line was installed. Coronal images (1 mm) were collated on a Signa 1.5T system (GE Healthcare Life Sciences, Piscataway, NJ). Images were T1-weighted and taken in three planes with a repetition time of 700 msec, an echo time of 20 msec, and a flip angle setting of 30°. A scanning time of approximately 20 min was employed, with a 15-cm field of view, a 192 matrix, and 2NEX (number of averages per signal unit). Each scan lasted approximately 20 min. The coronal MRI images were used to determine the three-dimensional structure of the caudate nucleus and the putamen, and surgical coordinates were generated from magnified coronal images (×1.5).

Stereotactic surgery and AAV2 infusion

All of the subjects in this study received bilateral infusions into both putamen and substantia nigra of either AAV2-GDNF or phosphate-buffered saline (PBS). Animals receiving putaminal AAV2-GDNF received PBS in the left putamen and bilateral PBS infusions in the substantia nigra. Animals treated with AAV2-GDNF in the right substantia nigra received PBS into the left substantia nigra and bilateral PBS infusions into the putamen. Animals treated with PBS only, received

bilateral PBS infusions into the putamen and substantia nigra. Infusions into the putamen (75 μl per site) were performed with CED at pre- and postcommissural levels; substantia nigra received a single (50 μl) infusion as previously described (Bankiewicz *et al.*, 2000; Hadaczek *et al.*, 2006a). Monkeys given putaminal infusions of vector received either a low dose (LD PUT; 1.1×10^{12} vg/ml, $n = 3$) or a high dose (HD PUT; 1.1×10^{13} vg/ml, $n = 5$) of AAV2-GDNF. A third group of monkeys ($n = 3$) received a high dose of AAV2-GDNF in the substantia nigra of the right hemisphere (SN). A fourth group of monkeys received PBS infusions only ($n = 3$). After infusion, the cannula was left in place for 5 min before it was retracted and then the scalp was closed with sutures.

Locomotor activity

Locomotor activity was measured by means of small portable physical activity monitors (Actical; Mini Mitter/ Respironics, Bend, OR). Monitors were enclosed in collars fitted on monkeys for a period of 2–3 weeks. These monitors contain an accelerometer to monitor the occurrence and intensity of movement at 1-min intervals. Total locomotor activity over the 12-hr day cycle was calculated for each day of assessment, and the mean across the assessment period was calculated. Values were collected before gene transfer, and twice in the 3 months after surgery.

Positron emission tomography methods and analysis

PET imaging with the aromatic L-amino acid decarboxylase (AADC)-specific probe, 6-[^{18}F]-fluoro-L-*m*-tyrosine (FMT), was performed as previously described (Eberling *et al.*, 1997), 3 months before (baseline) and 3 months after vector infusion. PET data were quantified by a multiple time graphical analysis (Patlak plot) with the time–activity curve for a region, the cerebellum, in which the tracer is nonspecifically bound as the input function. Asymmetry ratios were calculated to assess differences between the contralateral (PBS) and ipsilateral (AAV2-GDNF or PBS) hemispheres. Comparisons were made between baseline and posttreatment asymmetry ratios with paired *t* tests.

Immunohistochemistry

For immunohistochemistry, midbrain blocks containing the substantia nigra or caudate nucleus and putamen were postfixed in Zamboni's fixative, and then cryoprotected in several changes of 30% sucrose in PBS. Once prepared, blocks were frozen in liquid nitrogen and stored at -80°C until further analyses. Serial 40-μm sections were collected at -17°C on a cryostat (HM500M; Microm, San Marcos, CA) and stored in a cryoprotective solution at 4°C. Every tenth section of caudate–putamen and substantia nigra was evaluated for tyrosine hydroxylase (TH) or GDNF immunoreactivity (IR) by chromogenic visualization. Sections were washed and nonspecific binding was blocked by incubation in normal serum for 1 hr followed by incubation overnight at 4°C with primary antibodies against TH (diluted 1:600; Chemicon International/Millipore, Billerica, MA) or GDNF (diluted 1:500; R&D Systems, Minneapolis, MN). Adjacent sections were stained with hematoxylin and eosin (H&E). IR was visualized after exposure to biotinylated antibodies (diluted 1:300; Vector Laboratories, Burlingame, CA) and streptavidin conjugated to horseradish peroxidase (diluted 1:300; Vector Laboratories) with diaminobenzidine (DAB) and hydrogen peroxide (Vector Laboratories). TH IR was optimized for cell counting and photodensity measurements on nigral and caudate–putamen sections, respectively.

As previously described (Krauze *et al.*, 2008), BrainLAB (Westchester, IL) software was used to estimate volumetric distribution of GDNF distribution in caudate–putamen through correlation of immunostaining on sequential sections with MRI data.

Photodensity of TH IR was measured by means of intensity difference values for the region of interest (ROI) compared with white matter. The DAB reaction was terminated at a point at which detection of changes in TH IR in striatal fibers is optimal, before optimal development time for visualizing IR in cytoplasm of striatal dopaminergic neurons. Fiber staining in such sections is too dark to allow accurate assessments of interhemispheric differences in optical density. Mean values were calculated for two or three sections per monkey. For each section, 100 sites were assessed in each region of interest.

For each monkey, TH-IR neurons in the SN were counted in 2 sections, 10 sections apart, by the optical fractionator technique (Stereo Investigator 7 software; MBF Biosciences, Chicago, IL). The SN was precisely outlined at low magnification ($\times 2.5$ objective) on a Zeiss Axioskop microscope (Carl Zeiss, Thornwood, NY). The counting frame of the optical fractionator was defined in 100-μm squares and the systematic sampling was performed with a sampling grid of 200-μm squares. The sample sites were automatically generated by the computer and examined with a $\times 100$ objective. The counting frame displays inclusion and exclusion lines. Only IR cell bodies with nucleoli falling within the inclusion area of the counting frame, and not in contact with the exclusion lines, were counted. In addition, the nucleolus was enumerated in the counting frame only if it came into focus within the predetermined optical dissector (8 μm), with a 2-μm guard zone set to the top of the section. Section thickness was monitored with a Zeiss Axioskop microcator.

GDNF enzyme-linked immunosorbent assay

Concentrations of GDNF were determined with a commercially available kit (Promega, Madison, WI). The limit of detection for this kit is approximately 30 pg/ml of tissue extract. Tissue punches (2×3 mm; 10–20 mg wet weight) were collected from SN, caudate–putamen, and other brain regions within areas of maximal GDNF IR. Samples were homogenized in 250 μl of lysis buffer with a Fisher Scientific model 100 sonic dismembrator (Thermo Fisher Scientific, Waltham, MA) supplemented with protease inhibitors (Protease Inhibitor Cocktail; Roche Molecular Biochemicals, Indianapolis, IN) and then centrifuged for 15 min at $13,000 \times g$ at 4°C. Standard, kit control, or samples were added to wells coated with antibody specific for GDNF. When necessary, the samples were diluted with loading buffer. After a 6-hr incubation, wells were washed thoroughly, and enzyme-linked polyclonal antibodies against GDNF were added to each well and allowed to incubate overnight. Plates were then washed and incubated with peroxidase-labeled secondary antibody for 2 hr. Substrate solution (SuperSignal; Pierce Biotechnology/Thermo Fisher Scientific, Rockford, IL) was then added to each well and plates were read after a 10-min incubation. Chemiluminescence, expressed as relative light units (RLU), was

TABLE 1. LEVELS OF GLIAL CELL-DERIVED NEUROTROPHIC FACTOR IN CAUDATE–PUTAMEN AND SUBSTANTIA NIGRA AFTER INFUSION OF AAV2-GDNF[a]

	PUT	CN	GPi	GPe	STN	THAL	SNc	SNr	VTA
LD PUT	++	++	X	X	+++	X	+	+	X
SN	++	++	+++	+++	+++	+++	+++	++	+++
HD PUT	+++	+++	+++	+++	++	++	++	+	X

Abbreviations: CN, caudate nucleus; Gpe, globus pallidus, external segment; GPi, globus pallidus, internal segment; HD PUT, high-dose putamen; LD PUT, low-dose putamen; PUT, putamen; SN, substantia nigra; SNc, substantia nigra pars compacta; SNr, substantia nigra pars reticulata; STN, subthalamic nucleus; THAL, thalamus; VTA, ventral tegmental area.

[a]Ratings of immunohistochemical visualization of GDNF are indicated as follows: X, absence of immunoreactivity (IR); +, <25% coverage of structure with a few scattered IR neurons or fibers, and pale staining intensity; ++, >25% to <50% coverage of structure; +++, >50% coverage of structure, GDNF-positive cells and fibers and extracellular IR, intense staining.

measured with an FLx800 microplate reader (BioTek Instruments, Winooski, VT). The concentration of GDNF in tissue extracts was then calculated by reference to a standard curve.

Analyses of dopamine and metabolites by high-performance liquid chromatography

Levels of DA, serotonin (5-HT), norepinephrine, epinephrine, and of metabolites of DA and 5-HT were determined with a high-performance liquid chromatography (HPLC) system as previously described (Johnston *et al.*, 2008). Briefly, alternate 3-mm brain blocks were immersed in isopentane solution chilled to $-80°C$ and then stored at $-80°C$. Free dissected tissue was collected from caudate–putamen within regions of maximal GDNF IR. These samples were placed immediately in $500\,\mu l$ of ice-cold $0.4\,M$ perchloric acid, sonicated, and centrifuged for 15 min at 13,000 rpm at $4°C$. Supernatant ($30\,\mu l$) was injected onto the HPLC system coupled to electrochemical detection (CoulArray 5600A; ESA, Chelmsford, MA) for measurement of DA and its metabolites, dihydroxyphenylacetic acid (DOPAC) and homovanillic acid (HVA), as well as 5-HT and its principal metabolite, 5-hydroxyindoleacetic acid (5-HIAA). Protein content was determined in pellet fractions according to the method of Lowry and colleagues (1951).

Statistical analyses

PET and locomotor data were analyzed by t test. All other data sets were analyzed by two-way analysis of variance (ANOVA) (Prism; GraphPad Software, La Jolla, CA). When significance was achieved, post-hoc comparisons were performed via one-way ANOVA with Newman–Keuls tests.

Differences between ipsilateral and contralateral sides were analyzed by Student paired t test. A statistically significant difference is defined as $p < 0.05$.

Results

FMT imaging and locomotor activity

PET imaging of the AADC substrate FMT (Eberling *et al.*, 2008) revealed that putaminal infusion of AAV2-GDNF exhibited a tendency ($p = 0.06$) to increase uptake within the ipsilateral putamen, irrespective of vector dose (Fig. 1A and B), in agreement with previously published findings with lentiviral GDNF constructs (Kordower *et al.*, 2000). The inset in Fig. 1A shows representative FMT-PET images 3 months before and after gene transfer. The small, statistically insignificant changes in FMT-PET in individual groups of animals could be eliminated by pooling all animals irrespective of vector dose or anatomic target, and Fig. 1B reveals a statistically significant ($p < 0.05$) increase in relative change in FMT-PET when the untreated left hemisphere is compared with the right. AAV2-GDNF treatment produced a statistically significant increase ($p < 0.05$) in locomotor activity only in the low-dose putamen group (Fig. 1, lower left panel), whereas the PBS control group ($n = 3$) experienced a decline ($p < 0.05$) in activity after surgery. Neither infusion of vector into substantia nigra (SN) nor a high dose of vector in putamen produced a significant increase. In the latter case, this lack of significance is attributed to a single outlier. However, a significant difference was evident once data were aggregated and represented as the difference in total activity between PBS and combined GDNF-treated groups (Fig. 1, lower right panel).

TABLE 2. QUANTIFICATION OF BRAIN GLIAL CELL-DERIVED NEUROTROPHIC FACTOR LEVELS AFTER INFUSION OF AAV2-GDNF TO PUTAMEN OR SUBSTANTIA NIGRA[a]

	PUT		CN		SN		FC	
	L	R	L	R	L	R	L	R
PBS	0	0	0	0	0	0	0	0
LD PUT	0	0.09	0	0.66	0	1.1	0	0.013
SN	0.07	2.12	0.08	10.16	0.18	11.82	0.03	2.67
HD PUT	0	27.32	0	1.49	0.07	9.58	0.04	0.74

Abbreviations: CN, caudate nucleus; FC, frontal cortex; HD PUT, high-dose putamen; L, left (contralateral); LD PUT, low-dose putamen; PBS, phosphate-buffered saline; PUT, putamen; R, right (ipsilateral); SN, substantia nigra.

[a]Measurements of GDNF by ELISA (see Materials and Methods). Values are expressed as nanograms of GDNF per milligram of tissue homogenate protein.
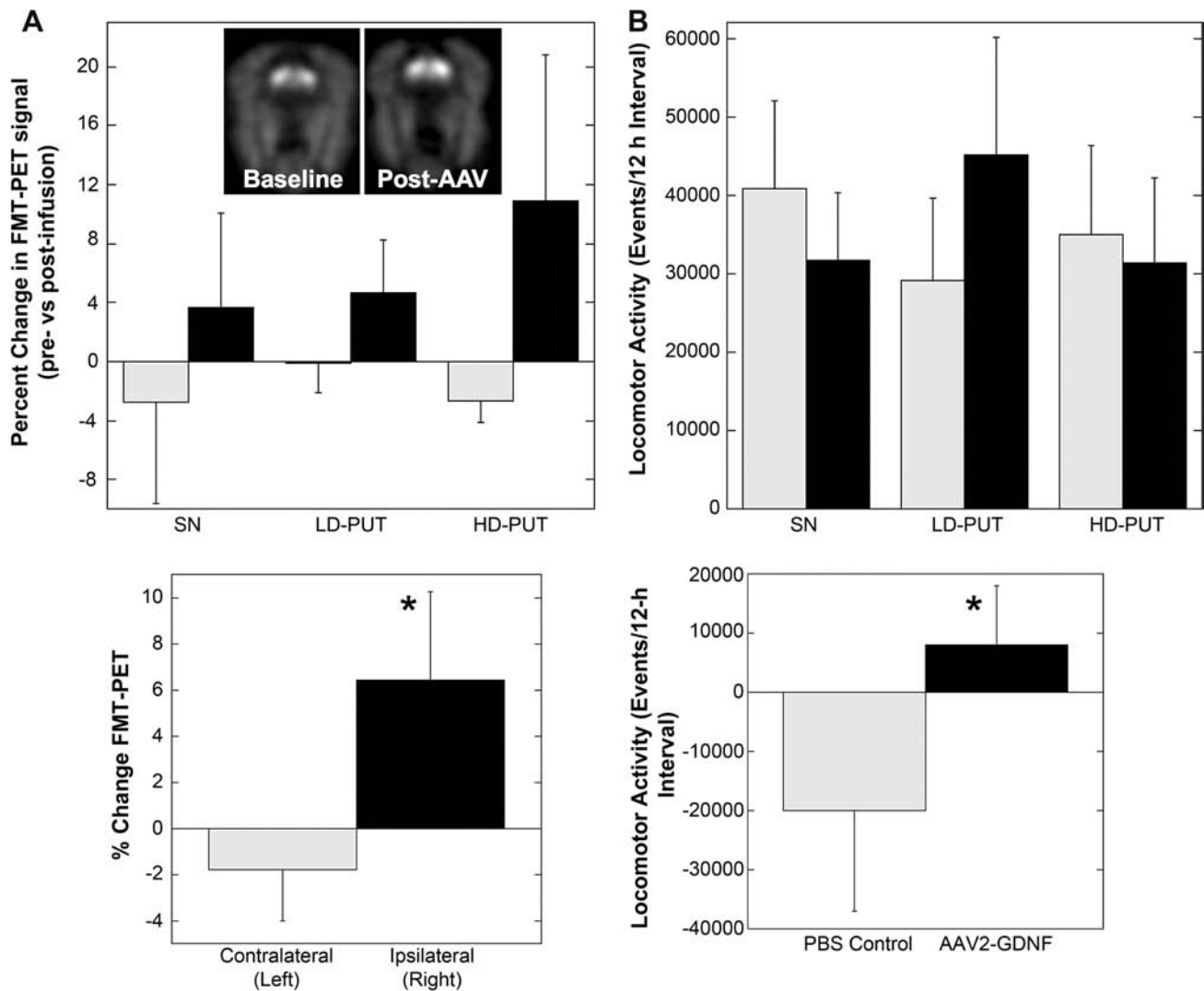
FIG. 1. Effect of AAV2-GDNF on FMI uptake and locomotor activity in aged monkeys. (**A**) Percent change in FMT-PET signal over baseline (pre-infusion) 3 months after AAV2-GDNF infusion in the left (contralateral, gray) vs. right (ipsilateral, black) striatum. *Inset:* Representative PET images from an animal that received a low dose of AAV2-GDNF in putamen. The ipsilateral infusion site is on the right in each image. A trend toward increased FMT-PET is evident in all three groups regardless of site of infusion or dose. When all animals were pooled (*lower left panel*), 2-way ANOVA revealed a significant effect of AAV2-GDNF infusion (*$p < 0.05$). (**B**) Locomotor activity, measured electronically over a 12-h daytime period at baseline (gray) and 6-months after surgery (black). When all the AAV2-GDNF treatment groups were pooled and changes from baseline activity were calculated (*lower right panel*), locomotor activity in the control group declined (gray), whereas AAV2-GDNF-treated animals (black) tended to have increased activity (*$p < 0.05$).

Pattern of GDNF protein expression

Putaminal infusions with AAV2-GDNF resulted in intense fiber and extracellular staining for GDNF within the putamen and caudate (Table 1 and Fig. 2A–C) that was not present in control tissues (left hemisphere in Fig. 2A–C). Figure 2A shows the extent of distribution of GDNF immunoreactivity in a representative coronal section from a monkey that received a high dose of AAV2-GDNF. For comparison, a circle has been superimposed that corresponds to the approximate diameter (10 mm) of a human putamen. On this basis, we predict that infusion of 75 μl of vector into human putamen should result in acceptable coverage of the target area. Figure

2B and C is representative of GDNF distribution after low-dose vector infusion into the putamen and substantia nigra, respectively. Infusion of AAV2-GDNF within the putamen produced a greater volume of GDNF immunoreactivity (IR) in the putamen compared with the caudate nucleus, irrespective of vector dose (see Table 3). But the resulting volume of distribution was 2-fold greater in the HD group, in agreement with the large difference in GDNF levels (Table 2). Delivery of vector into the substantia nigra generated stronger GDNF expression in the caudate nucleus than was seen with either dose of vector in the putamen. The notation "HD" in Fig. 2C indicates that the dose of vector delivered to SN was the same as for the high-dose putamen group.
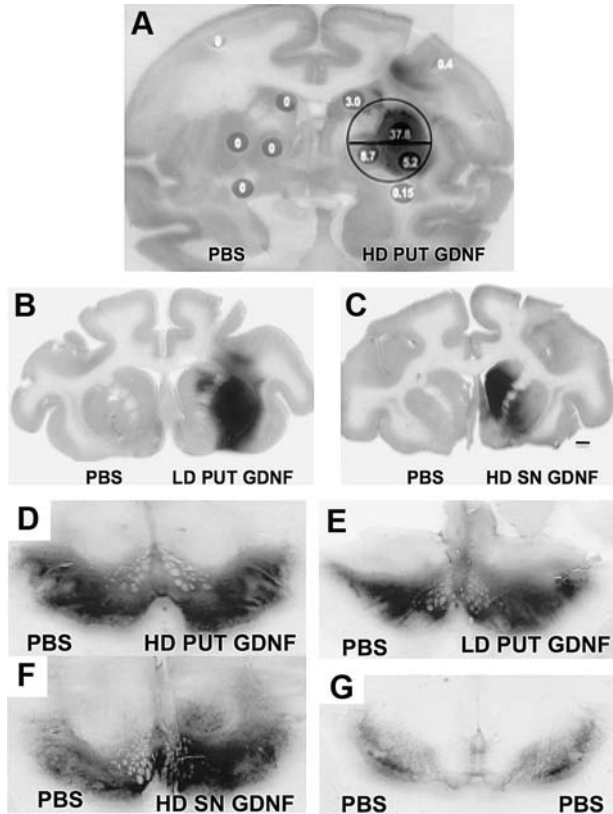
FIG. 2. Effect of infusion site and vector dose on immuno-histochemical distribution of GDNF protein and nigral TH staining. (**A**) Infusion of 75 μl of AAV2-GDNF into monkey putamen produced extensive expression of GDNF in putamen. The circle represents the approximate diameter of a human putamen for comparison (10 mm). The numbers in the gray dots indicate the concentration of GDNF, expressed as nanograms per milligram of protein. This section is from a monkey that received a high putaminal dose of AAV2-GDNF. (**B**) Low-dose (LD) AAV2-GDNF to putamen. (**C**) High dose of vector delivered to the SN. Note the prominent caudal staining. (**D–G**) Effect of AAV2-GDNF on nigral TH staining. GDNF expression increased TH staining independent of site (putamen or SN). HD increased TH more than did LD. Black bar in panel 2C represents a 2-mm segment applicable to panels B–G. The circle in panel A represents a 10-mm diameter centered on the infusion site.

Tyrosine hydroxylase (TH) staining of nigral neurons (Fig. 2D–G) indicated significant upregulation of TH activity irrespective of vector dose or anatomical location. Contralateral upregulation was evident in all vector-treated animals, due presumably to decussation of nigral neurons (Douglas *et al.*, 1987). GDNF immunoreactivity was also seen in the subthalamic nucleus (STN) and globus pallidus (GP) after HD infusions of AAV2-GDNF to the putamen, with IR fibers also observed in these nuclei (Table 1). This result indicates anterograde and retrograde transport of GDNF protein (Parent *et al.*, 1995). In HD putamen monkeys, there was a gradient of GDNF concentration around the infusion site.

Nigral infusions of the vector produced nanogram levels of GDNF, intense GDNF staining in the striatum, and a greater volume of distribution in the caudate nucleus versus the pu-

TABLE 3. VOLUME OF DISTRIBUTION MEASUREMENTS FOR GLIAL CELL-DERIVED NEUROTROPHIC FACTOR IMMUNOREACTIVITY AFTER INFUSION OF AAV2-GDNF TO PUTAMEN OR SUBSTANIA NIGRA[a]

	PUT	CN
LD PUT	139 ± 72.8	16.0 ± 16.3
SN	200 ± 73.7	339 ± 76.2
HD PUT	285 ± 22.5	31.0 ± 5.45

Abbreviations: CN, caudate nucleus; HD PUT, high-dose putamen; LD PUT, low-dose putamen; PUT, putamen; SN, substantia nigra.
[a]Mean ($\pm$SEM) volume measurements are reported as cubic millimeters.

tamen (Tables 2 and 3; and Fig. 2C). This finding demonstrates anterograde transport of large amounts of GDNF protein to the terminal fields of the nigrostriatal pathway. GDNF was also seen in the cytoplasm of neurons and fibers within the SN, ventrotegmental area (VTA), GP, and STN (Fig. 2G). Greater staining was observed in neurons of the compacta versus those in the reticulata region of the SN, whereas greater fiber staining occurred in the latter compartment. The morphology, density, and neuroanatomical localization of IR cells in the SNc suggest that these neurons are dopaminergic.

Measurement of GDNF protein levels in the aged macaque brain

To quantify GDNF expression that occurs *in vivo* after infusion of AAV2-GDNF to the nigrostriatal system, we measured levels of the growth factor 6 months after AAV2-GDNF delivery by ELISA. GDNF was not detected in cerebrospinal fluid or blood plasma (data not shown). GDNF levels were

TABLE 4. ASYMMETRY IN NEUROTRANSMITTER LEVELS INDUCED BY ELEVATED LEVELS OF GDNF IN THE PUTAMEN OF AGED MONKEYS[a]

|	PBS	LD PUT	SN	HD PUT
5-HT	100	222	**182***	104
5-HIAA	106	**179***	150	127
NE	128	177	**194***	243
EPI	133	67	**265***	135

Abbreviations: 5-HIAA, 5-hydroxyindoleacetic acid; 5-HT, serotonin; EPI, epinephrine; HD PUT, high-dose putamen; LD PUT, low-dose putamen; NE, norepinephrine; PBS, phosphate-buffered saline (control); SN, substantia nigra.
[a]Data are expressed as a percentage of the relevant value determined in the contralateral hemisphere. Asterisk indicates a statistically significant difference ($p < 0.05$) of data compared with the PBS control group. Statistical analysis was performed by two-way ANOVA, followed by one-way and Newman–Keuls post-hoc analyses. 5-HT: two-way ANOVA, significant effect of treatment ($p < 0.05$) irrespective of hemisphere. Overall, SN treatment was associated with higher putaminal 5-HT than other treatment groups. 5-HIAA: two-way ANOVA, significant effect of hemisphere ($p < 0.05$). LD PUT treatment increased 5-HIAA levels compared with PBS group. Norepinephrine (NE): two-way ANOVA, significant effect of hemisphere ($p < 0.05$). SN treatment was associated with higher NE levels in both hemispheres. Epinephrine (EPI): two-way ANOVA, significant effect of treatment ($p < 0.05$), irrespective of hemisphere.

measured in discrete tissue punches chosen on the basis of GDNF IR (Table 2). The mean level of GDNF expressed by AAV2-GDNF in the putamen was 0.09, 2.12, and 27.2 ng/mg in the LD putamen, HD putamen, and SN groups, respectively. GDNF was higher than control values in two of the three monkeys given LD putamen treatment. GDNF levels in the caudate nucleus were 0.66, 10.16, and 21.77 ng/mg in the LD putamen, SN, and HD putamen groups, respectively. GDNF was above control values in the caudate nucleus of two of three monkeys assessed in the LD putamen group. Individual levels of GDNF in the SN were 1.1, 11.8, and 9.6 ng/mg in the LD putamen, SN, and HD putamen groups, respectively. Here, GDNF could be quantitated only in one monkey out of the four evaluated after LD putamen treatment. After AAV2-GDNF infusion, GDNF was detected at low levels in other brain regions including the frontal cortex and white matter in the cortex (Table 2). GDNF was not detected in PBS control animals in any brain region.
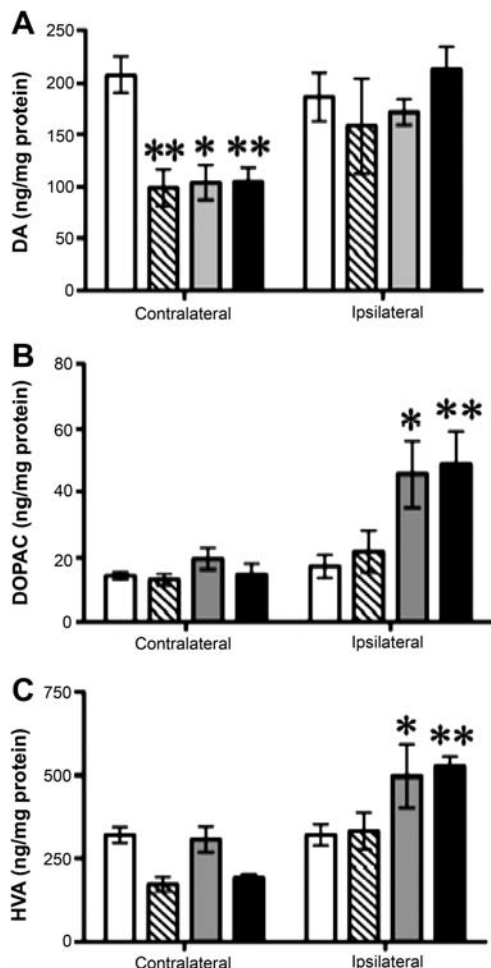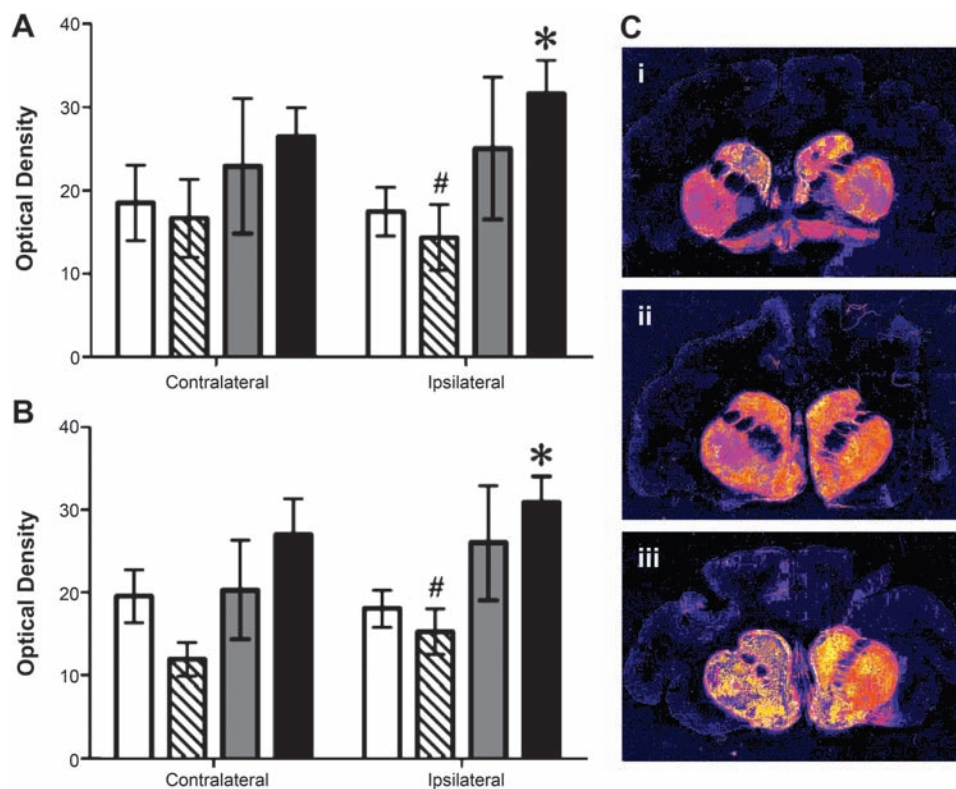

FIG. 3. Effect of GDNF on dopamine and principal metabolites in the putamen. Open columns, control animals that received a PBS infusion; hatched columns, low-dose putamen group; gray columns, substantia nigra group; solid columns, high-dose putamen group. Statistical indicators are as follows: *$p < 0.05$, **$p < 0.01$, two-way ANOVA, followed by one-way ANOVA post-hoc tests, and Newman–Keuls post-hoc comparisons with PBS group.
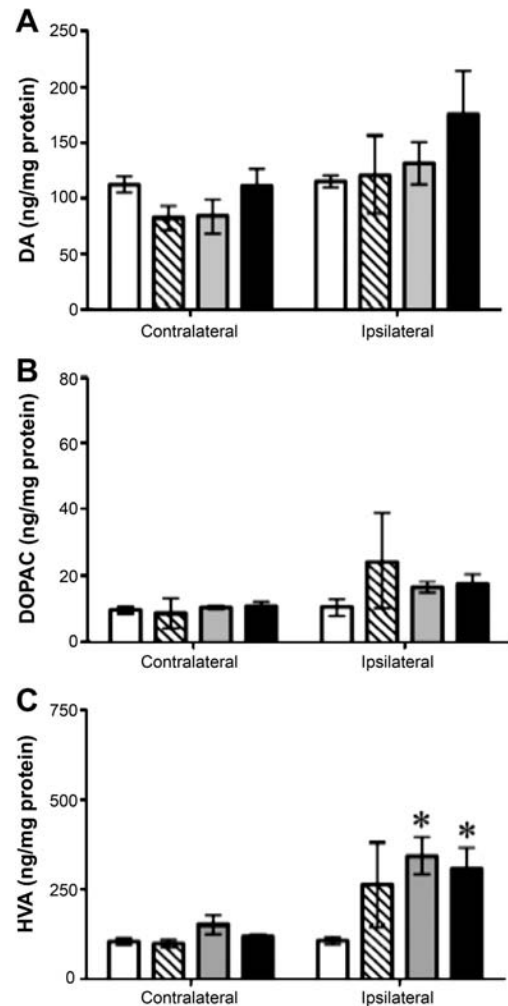
FIG. 4. Effect of GDNF on dopamine and metabolites in the caudate nucleus. Open columns, control animals that received a PBS infusion; hatched columns, low-dose putamen group; gray columns, substantia nigra group; solid columns, high-dose putamen group. Statistical indicators are as follows: *$p < 0.05$, two-way ANOVA, followed by one-way ANOVA post-hoc tests and Newman–Keuls post-hoc comparisons with PBS control.

Striatal neurochemistry

To determine whether GDNF expression altered the concentration of catecholamines, serotonin, and their metabolites, we performed HPLC analyses of samples from the putamen and caudate nucleus of monkeys that had received infusion of AAV2-GDNF 6 months previously. Within the ipsilateral putamen and caudate nucleus, DA concentration was comparable to PBS control values (Figs. 3A and 4A). However, in the contralateral putamen, DA levels decreased significantly in all AAV2-GDNF treatment groups on the contralateral side. Infusion of a high dose of vector, either to the SN or PUT, significantly increased the concentration of DOPAC and HVA on the ipsilateral side (Fig. 3B and C, respectively) relative to control (PBS) infusion. These changes suggest a persistent increase in DA turnover in response to expression of human GDNF protein within the aged nigrostriatal pathway. In

FIG. 5. Tyrosine hydroxylase immunoreactivity in the putamen after infusion of AAV2-GDNF to the putamen. Open columns, control animals that received a PBS infusion; hatched columns, low-dose putamen group; gray columns, substantia nigra group; solid columns, high-dose putamen group. Columns and error bars represent mean ($\pm$SEM) optical density measurements (relative to white matter). (**A**) Putamen: Two-way ANOVA revealed a significant interaction between hemisphere and treatment ($p < 0.05$); unpaired post-hoc test for right side: PBS versus high-dose putamen, $p < 0.05$; one-way ANOVA, $p < 0.05$. Post-hoc analyses by unpaired t tests indicated a significant difference between PBS and high-dose putamen treatment groups (*$p < 0.05$). In addition, mean optical density in the low-dose putamen group was significantly less than that measured in the high-dose putamen group ($^{\#}p < 0.05$). (**B**) Caudate nucleus: Two-way ANOVA revealed a significant effect of side ($p = 0.02$); one-way ANOVA ($p < 0.01$). Unpaired t tests (one-tailed): PBS versus HD putamen treatment (*$p < 0.05$), LD putamen versus HD putamen ($^{\#}p < 0.01$). (**C**) False color TH staining of representative sections from (i) LD putamen, (ii) SN, and (iii) HD putamen.

contrast to the dose- and site-independent effects of AAV2-GDNF on DA and its metabolites, only the SN treatment significantly increased levels of 5-HT and norepinephrine (NE) in the putamen when the left hemisphere is compared with right (Table 4). In a number of cases, larger mean percentage increases were not statistically significant because of wide variation in individual measures.

Striatal fiber density analysis

Because viral vectors containing GDNF transgenes have been shown to downregulate TH in both the intact and 6-hydroxydopamine (6-OHDA)-lesioned striatum of rats, we determined whether this was also the case in the AAV2-GDNF-treated caudate–putamen of the monkey (Georgievska *et al.*, 2002, 2004). Measurements were made on 2 or 3 sections, 10 sections apart, selected on the basis of their position within the axis of maximal staining intensity for GDNF in the caudate–putamen. Optical density of DAB precipitate was determined on striatal sections processed for TH immunohistochemistry, and quantified against standard optical density filters. HD putamen infusions increased the density of

dopaminergic terminals in ipsilateral putamen (Fig. 5A) and caudate nucleus (Fig. 5B). This indicates increased density of TH-IR fibers within these regions in response to HD putamen treatment, because these sections were developed specifically for detection of differences in fiber staining. Figure 5C shows false color staining for TH in representative sections from animals in each treatment group. Figure 5C (panel i) represents LD putamen and indicates a slight increase in TH staining in the right hemisphere, both caudal and putaminal. The corresponding numerical data in Fig. 5A indicate, however, that this was not a consistent increase across all animals in this group. Figure 5C (panel ii) suggests that infusion of AAV2-GDNF into ipsilateral (right) substantia nigra produced TH increases in both putamen and caudate, although interanimal variability resulted in insignificant differences in comparison with PBS data or with the contralateral hemisphere. The strongest increase in TH staining was caused by infusion of a high dose of AAV2-GDNF into the putamen as shown in Fig. 5C (panel iii). Moreover, an increase in contralateral TH can be discerned when compared with LD putamen (Fig. 5C, panel i). This impression was confirmed numerically in Fig. 5A and B, where statistically significant
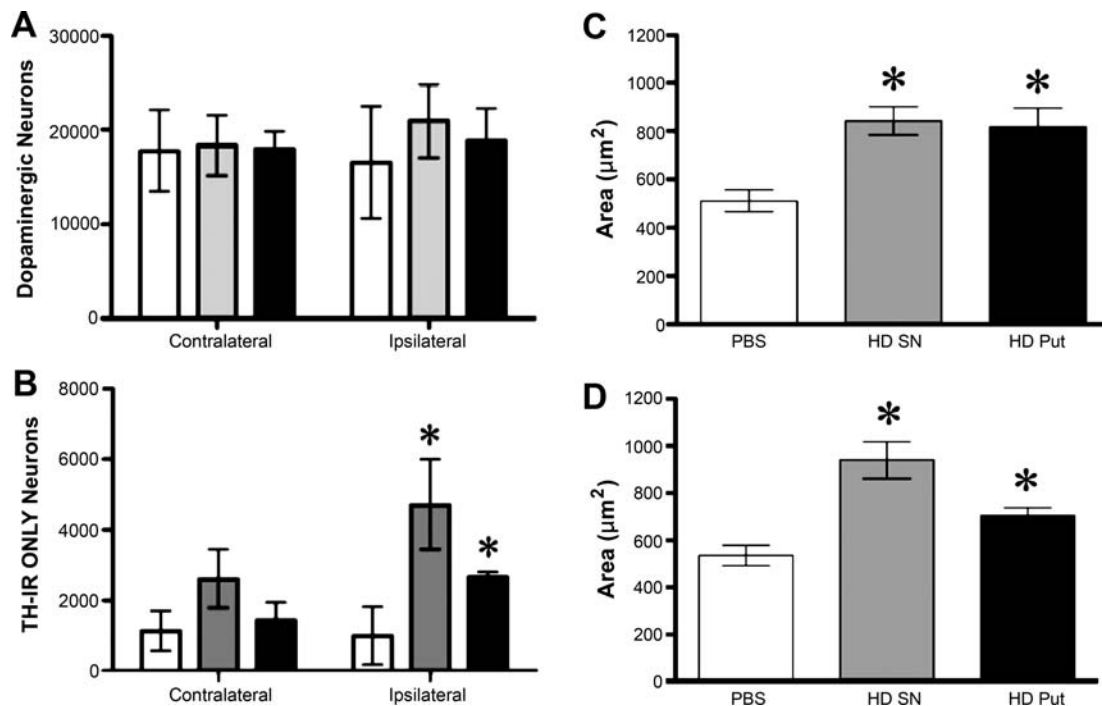
FIG. 6. Effect of high-dose GDNF on nigral neurons. Sections from animals that received either PBS (open columns), a high dose of AAV2-GDNF in SN (gray columns), or an equivalent dose in putamen (solid columns) were subjected to stereology (see Materials and Methods). Cells were counted in 2 sections, 10 sections apart, at the level of the third nerve rootlets. (**A**) Total population of dopaminergic (TH) neurons. (**B**) Number of TH-containing nigral neurons after high-dose vector treatment. This subset of neurons does not contain neuromelanin deposits (TH-IR ONLY). (**C**) Vector treatment also increased cell body area (μm^2) in nigral dopaminergic neurons containing both TH and neuromelanin or in neurons containing neuromelanin only (**D**). The cell body of neurons containing either TH only or Nissl neurons without TH or neuromelanin did not increase in size. Statistical analysis: *$p < 0.05$, two-way ANOVA, followed by one-way ANOVA post-hoc tests, and Newman–Keuls post-hoc comparisons with PBS control.

increases between LD and HD treatment, and between PBS and HD treatment, were observed.

Dopaminergic neurons in the substantia nigra

Cell counting of dopaminergic neurons in the SN revealed the absence of neurodegeneration or neurogenesis after AAV2-GDNF infusions (Fig. 6A). Dopaminergic neurons can be classified into three groups based on the presence of TH and neuromelanin (NM) deposits (McCormack *et al.*, 2004). The data indicate that there were no effects (data not shown) on either the neurons that contained NM only, or on neurons that contained both TH and NM (TH/NM). However, neurons containing TH but no NM in their cytoplasm increased in number in the ipsilateral SN after AAV2-GDNF treatment (Fig. 6B). No significant increase was observed in the contralateral hemisphere. In contrast, high-dose vector increased cell body area in both TH/NM (Fig. 6C) and TH-only neurons (Fig. 6D). The fact that AAV2-GDNF increased the number of TH-only neurons suggests a strong upregulation of TH in neurons that did not previously express detectable levels, as opposed to TH/NM neurons that presumably represent constitutively active dopaminergic neurons.

In addition, GDNF overexpression (Fig. 7) induced sprouting of nigral and medial forebrain neurons as well as upregulation of TH staining. Although GDNF effects were more pronounced in the ipsilateral, GDNF-dosed hemisphere

(Fig. 7B and C), effects could also be seen in the contralateral hemisphere (Fig. 7A and B). Although it is not apparent why this should occur, we suspect that it may be due to decussation of nigral neurons to the contralateral hemisphere.

Discussion

Our findings demonstrate that aged nonhuman primates show improvement in several clinically relevant measures of nigrostriatal function in response to AAV2-GDNF. These monkeys represent a model of the aged human brain rather than parkinsonism, although aging is an important risk factor for PD. Accordingly, because gene therapy for PD is likely to be administered to older individuals, our study is confirmation of AAV2-GDNF vector safety in a relevant population of monkeys.

Normal aging is associated with declines in nigrostriatal and motor function (Pakkenberg *et al.*, 1995; McCormack *et al.*, 2004). We examined FMT uptake to determine whether AAV2-GDNF induces persistent downregulation of DA production *in vivo*, as found by others (Rosenblad *et al.*, 2003; Georgievska *et al.*, 2004). In the contralateral putamen that did not receive AAV2-GDNF, there was no change in FMT signal over the course of the study; this is interesting given the decrease in striatal dopamine seen in this hemisphere after ipsilateral administration of AAV2-GDNF. In the ipsilateral putamen, there was an increase relative to the contralateral
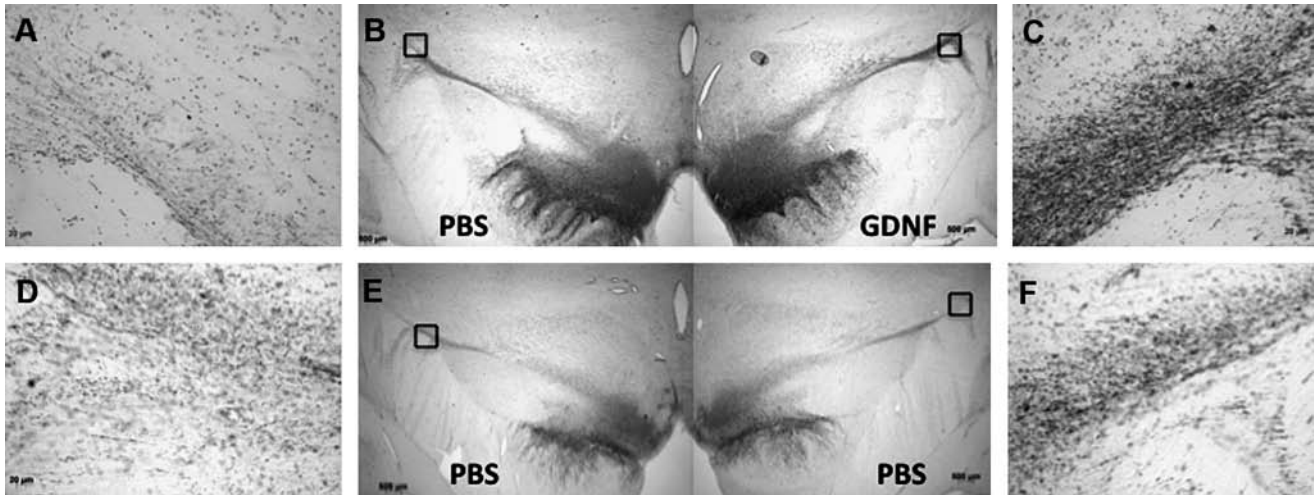
FIG. 7. Composite figure of TH IR showing midbrain region containing SN and MFB (medial forebrain bundle). Shown is TH staining of a representative nonhuman primate that received high-dose AAV2-GDNF administration into the right putamen (**A–C**) compared with a control animal (**D–F**) that received a PBS infusion into the right putamen. (**B**) and (**E**) clearly show GDNF-induced upregulation of dopaminergic neurons in the SNc and sprouting of TH-IR fibers in the MFB in this GDNF-treated animal. Upregulation appears to be bilateral, probably because of cross-over of GDNF to the contralateral hemisphere in line with contralateral effects on DA levels and fiber density (Figs. 3 and 5). In contrast, the PBS-treated animal indicates the normal appearance of dopaminergic cells in the SNc and TH-IR fibers in the MFB. Scale bars: (**B** and **E**) 500 μm; (**A, C, D**, and **F**) 20 μm.

side in monkeys that had received putaminal infusions of vector. Unilateral AAV2-GDNF treatment also altered basal locomotor activity, indicated by an increase in total daily activity relative to PBS monkeys. It is important to consider that FMT uptake reflects AADC rather than TH activity, and AADC expression typically does not decline with age (DeJesus *et al.*, 2001). However, our findings suggest that elevated GDNF in the striatum induced a small increase in AADC activity within the aged putamen and enhanced locomotor activity, which suggest improved dopaminergic activity.

Age-related motor deficits have been reported in both rodents and nonhuman primates (Walton *et al.*, 2006; Sanchez *et al.*, 2008). Portable activity monitors (PAMs) offer a noninvasive and objective means of assessing gross locomotor movements, and are widely employed in medical research. Unlike laboratory-based, observational methods of assessing locomotor activity, PAMs monitor activity in the baseline or "resting" conditions via small accelerometers sensitive to movement of the animal. Their measurements indicate whole body movements, correlate with activity counts, and are not affected by arm or head movements (Papailiou *et al.*, 2008). In our study, there was a decline in locomotor activity over a 6-month period in control rhesus macaques, but AAV2-GDNF attenuated this decline in dopaminergic functioning of the nigrostriatal pathway.

In our study, HD AAV2-GDNF treatments increased DA turnover in the putamen and caudate nucleus on the ipsilateral side. In contrast, DA levels in the contralateral putamen were decreased in all vector groups compared with PBS controls, similar to the change in FMT-PET signal observed in this hemisphere. In line with this finding is the observation of increased density of TH-IR fibers in the ipsilateral putamen after HD putamen treatment. A similar trend was also apparent after SN infusion. These data concur with clinical ev-

idence that GDNF can induce sprouting of dopaminergic terminals in the parkinsonian putamen (Love *et al.*, 2005). On the basis of these findings, one may compare the effects of GDNF with those of nerve growth factor (NGF) in the septohippocampal system of the rat. After fimbria–fornix lesioning, NGF infusions can prevent the subsequent decrease in choline acetyltransferase expression normally seen within cholinergic septal cells (Hoffman *et al.*, 1990). Similar to the ability of GDNF to induce sprouting of TH-containing terminals, NGF induces neurite extension. On the basis of morphology seen in the present study, it is unlikely these TH extensions are dystrophic terminals (data not shown) as previously documented in rat striata exposed to high levels of GDNF (Suwelack *et al.*, 2004).

Safety evaluation was the main objective in this study. Hence, infusion parameters for vector treatments are similar to those we would employ for delivery to the human brain. Indeed, a similar AAV2 striatal infusion is already being used in humans in a phase 1 study of AAV2-hAADC (Eberling *et al.*, 2008). This clinical study itself was based on extensive efficacy (Bankiewicz *et al.*, 2006; Forsayeth *et al.*, 2006) and safety (Sanftner *et al.*, 2004; Cunningham *et al.*, 2008) studies. In particular, Cunningham and colleagues (2008) showed that even quite large putaminal doses of AAV2 resulted in a remarkable degree of sequestration within the target and did not escape into peripheral tissues or trigger strong immune responses in nonhuman primates. Infusion of AAV2-GDNF by CED resulted in widespread, intense distribution around the site of infusion for high-dose treatments. The volume of GDNF distribution measured in these monkeys is considered to be adequate when considering human application. Site of vector infusion determined the pattern of GDNF IR in the caudate–putamen as putamen infusions produced greater coverage in the putamen than in the caudate nucleus, and the

reverse occurred after SN infusions. However, the difference in volume of distribution between these sites in the SN group was small. The volume of transgene IR seen in the putamen was equivalent to that seen in human brain with AAV2-hAADC, now in a clinical trial for PD (Eberling *et al.*, 2008). It is also apparent that delivery to SN produced only slightly reduced distribution of GDNF in the putamen, similar to that seen after putaminal delivery of the same dose. However, a survey of GDNF levels in tissue punches taken from regions of high IR in the putamen showed that a 10-fold greater concentration was achieved when the vector was delivered to the putamen. However, within the SN, mean GDNF levels were similar to those seen after putaminal infusions of the high dose of vector, indicating efficient retrograde axonal transport of GDNF.

Immunohistochemistry for GDNF revealed significant anterograde and retrograde transport of GDNF after HD treatments (Table 1). This is expected given the neurotropic profile of AAV2-GDNF constructs and the afferent and efferent connections to the regions infused (Parent *et al.*, 1995). Immunoreactivity was not observed in the contralateral hemisphere, despite picogram levels of GDNF in some regions. Given the reduction of DA in contralateral putamen after HD treatments, it was possible that GDNF might be found in the cerebrospinal fluid (CSF). This is not supported by our ELISA analysis of CSF samples, where GDNF levels were below the assay's limit of detection (30 pg/mg protein). Even with this limitation, detectable levels of GDNF were observed in contralateral putamen, caudate, SN, and frontal cortex of monkeys that had received SN infusions. In HD putamen monkeys, this occurred only in the SN and frontal cortex. In the LD putamen group, GDNF levels were much lower than in the HD groups. Control levels of GDNF reported by others are in the range of 5–8 pg/mg in control aged rhesus monkeys, which explains the apparent absence of GDNF in our PBS controls (Collier *et al.*, 2005). GDNF might also be anterogradely transported to the contralateral hemisphere in decussation (cross-over) nigrostriatal fibers (Morgan and Curran, 1986). Lower levels of GDNF were found in association with decreased DA in the contralateral putamen, whereas higher levels in the ipsilateral putamen occurred with an increase in DA turnover. Contralateral decrease in DA was also seen in the LD putamen group; yet turnover was not increased in the ipsilateral putamen. This suggests that the ability of GDNF to increase DA turnover is dose related.

Treatment of the SN with AAV2-GDNF also led to an increase in 5-HT and epinephrine in the ipsilateral putamen, consistent with know effects of GDNF on serotonin synthesis (Beck *et al.*, 1996) and expression of GDNF receptors on serotonergic neurons (Sarabi *et al.*, 2003). These changes are dependent on site of infusion, as they were not observed after putaminal infusions. This difference could offer additional benefits as 5-HT is known to interact with dopamine and norepinephrine to facilitate locomotor activity (Munoz *et al.*, 2003). There was also a trend toward increase in norepinephrine after both HD vector treatments (SN and putamen). Where putaminal GDNF levels were in the nanogram range, as seen after HD treatments, there was an increase in norepinephrine (NE) release. This finding is consistent with the observed increase in dopamine turnover measured in the ipsilateral putamen, as NE plays a stimulatory role in the release of dopamine from striatal terminals (Lategan *et al.*, 1992), and

is also consistent with the finding that neurturin, a GDNF homolog, stimulates neuritogenesis in locus ceruleus (LC) neurons (Holm *et al.*, 2002). In fact, there is evidence that norepinephrine may play a more significant role in PD than previously appreciated. In rodent PD models, loss of NE exacerbates both MPTP (Rommelfanger *et al.*, 2007) and 6-OHDA toxicity. The Braak hypothesis (Braak and Braak, 2000) describes the pathoanatomy of PD as an ascending disease in which gastric wall (vasoactive intestinal peptide [VIP]-positive) neurons degenerate early in the disease, followed by cardiac sympathetic neurons, brainstem nuclei such as in the LC, and finally SN neurons. Because NE itself is a free radical scavenger that also has receptor-mediated antiinflammatory effects (Rommelfanger and Weinshenker, 2007), loss of the LC may be a critical stage in the progressive loss of nigral neurons. On this basis, trophic effects of GDNF on catecholaminergic neurons rather than just dopaminergic neurons may improve symptoms in nonmotor aspects of PD as well.

The decrease in dopamine seen in the contralateral putamen is likely not due to downregulation of TH expression in nigrostriatal neurons, because we found that HD vector treatment increased the number of nonpigmented TH-IR neurons in the ipsilateral SN compared with PBS. At the same time, the number of such neurons in the contralateral SN was not different from the number in PBS monkeys, and the density of TH-IR fibers in the contralateral putamen after HD treatments was not reduced in comparison with that seen in PBS monkeys. This is in line with previously published results (Kordower *et al.*, 2000). Although not determined here, it is likely that TH activity is increased in both hemispheres (Eslamboli *et al.*, 2005). In response to chronically high levels of GDNF, TH enzymatic activity appears to be persistently upregulated in monkeys, whereas downregulation occurs in the rodent. Our cell-counting data show the absence of either neurodegeneration or neurogenesis in the total number of dopaminergic neurons at the level of the third nerve rootlets. However, there was a shift in phenotype: the percentage of nonpigmented dopaminergic (TH only) neurons increased after HD vector treatments. This is an interesting finding as it is this subpopulation that normally decreases with age, whereas the number of pigmented neurons increases (McCormack *et al.*, 2004). In addition, dopaminergic nigral neurons decrease in volume with advancing age (Chen *et al.*, 2000). Within the ipsilateral SN, our study found an increase in cell body area of pigmented dopaminergic neurons, in response to HD vector treatments, suggesting increased cellular function in line with the increase in dopamine turnover seen in the putamen.

In conclusion, the present study suggests that, even when nonhuman primates are intentionally overdosed with AAV2-GDNF, no overt toxicity can be detected and that aged primates tolerate the procedure well; a separate report dealing specifically with neuropathology in these animals is in preparation. In addition, we saw several encouraging indicators of a potential efficacious effect on the dopaminergic system in these animals that may be supported by direct efficacy studies in stable MPTP-treated monkeys underway now (Eberling *et al.*, 2009).

Acknowledgments

Author Disclosure Statement

No competing financial interests exist.

References

Airaksinen, M.S., and Saarma, M. (2002). The GDNF family: Signalling, biological functions and therapeutic value. Nat. Rev. Neurosci. 3, 383–394.

Bankiewicz, K.S., Eberling, J.L., Kohutnicka, M., Jagust, W., Pivirotto, P., Bringas, J., Cunningham, J., Budinger, T.F., and Harvey-White, J. (2000). Convection-enhanced delivery of AAV vector in parkinsonian monkeys: *In vivo* detection of gene expression and restoration of dopaminergic function using prodrug approach. Exp. Neurol. 164, 2–14.

Bankiewicz, K.S., Forsayeth, J., Eberling, J.L., Sanchez-Pernaute, R., Pivirotto, P., Bringas, J., Herscovitch, P., Carson, R.E., Eckelman, W., Reutter, B., and Cunningham, J. (2006). Long-term clinical improvement in MPTP-lesioned primates after gene therapy with AAV-hAADC. Mol. Ther. 14, 564–570.

Beck, K.D., Irwin, I., Valverde, J., Brennan, T.J., Langston, J.W., and Hefti, F. (1996). GDNF induces a dystonia-like state in neonatal rats and stimulates dopamine and serotonin synthesis. Neuron 16, 665–673.

Berheimer, H., Birkmayer, W., Hornykiewics, O., Jellinger, K., and Seitelberger, F. (1973). Brain dopamine and the syndromes of Parkinson and Huntington: Clinical, morphological and neurochemical correlations. J. Neurol. Sci. 20, 415–455.

Braak, H., and Braak, E. (2000). Pathoanatomy of Parkinson's disease. J. Neurol. 247(Suppl. 2), II3–II10.

Chen, E.Y., Kallwitz, E., Leff, S.E., Cochran, E.J., Mufson, E.J., Kordower, J.H., and Mandel, R.J. (2000). Age-related decreases in GTP-cyclohydrolase-I immunoreactive neurons in the monkey and human substantia nigra. J. Comp. Neurol. 426, 534–548.

Collier, T.J., Dung Ling, Z., Carvey, P.M., Fletcher-Turner, A., Yurek, D.M., Sladek, J.R., JR., and Kordower, J.H. (2005). Striatal trophic factor activity in aging monkeys with unilateral MPTP-induced parkinsonism. Exp. Neurol. 191(Suppl. 1), S60–S67.

Cunningham, J., Pivirotto, P., Bringas, J., Suzuki, B., Vijay, S., Sanftner, L., Kitamura, M., Chan, C., and Bankiewicz, K.S. (2008). Biodistribution of adeno-associated virus type-2 in nonhuman primates after convection-enhanced delivery to brain. Mol. Ther. 16, 1267–1275.

DeJesus, O.T., Endres, C.J., Shelton, S.E., Nickles, R.J., and Holden, J.E. (2001). Noninvasive assessment of aromatic ʟ-amino acid decarboxylase activity in aging rhesus monkey brain *in vivo*. Synapse 39, 58–63.

Douglas, R., Kellaway, L., Mintz, M., and Van Wageningen, G. (1987). The crossed nigrostriatal projection decussates in the ventral tegmental decussation. Brain Res. 418, 111–121.

Eberling, J.L., Bankiewicz, K., Jordan, S., Vanbrocklin, H.F., O'Neil, J.P., Emborg, M., and Jagust, W. (1997). PET [¹⁸F]6-fluoro-ʟ-*m*-tyrosine imaging of MPTP-lesioned primates. Brain Res. 750, 264–276.

Eberling, J.L., Jagust, W.J., Christine, C.W., Starr, P., Larson, P., Bankiewicz, K.S., and Aminoff, M.J. (2008). Results from a phase I safety trial of hAADC gene therapy for Parkinson's disease. Neurology 70, 1980–19893.

Eberling, J.L., Kells, A.P., Pivirotto, P., Beyer, J., Bringas, J., Federoff, H.J., Forsayeth, J., and Bankiewicz, K.S. (2009). Functional effects of AAV2-GDNF on the dopaminergic nigrostriatal pathway in Parkinsonian rhesus monkeys. Hum. Gene Ther. 20, 511–518.

Emborg, M.E., Ma, S.Y., Mufson, E.J., Levey, A.I., Taylor, M.D., Brown, W.D., Holden, J.E., and Kordower, J.H. (1998). Age-related declines in nigral neuronal function correlate with motor impairments in rhesus monkeys. J. Comp. Neurol. 401, 253–265.

Eslamboli, A., Georgievska, B., Ridley, R.M., Baker, H.F., Muzyczka, N., Burger, C., Mandel, R.J., Annett, L., and Kirik, D. (2005). Continuous low-level glial cell line-derived neurotrophic factor delivery using recombinant adeno-associated viral vectors provides neuroprotection and induces behavioral recovery in a primate model of Parkinson's disease. J. Neurosci. 25, 769–777.

Fiandaca, M., Forsayeth, J., and Bankiewicz, K. (2008). Current status of gene therapy trials for Parkinson's disease. Exp. Neurol. 209, 51–57.

Forsayeth, J.R., Eberling, J.L., Sanftner, L.M., Zhen, Z., Pivirotto, P., Bringas, J., Cunningham, J., and Bankiewicz, K.S. (2006). A dose-ranging study of AAV-hAADC therapy in parkinsonian monkeys. Mol. Ther. 14, 571–577.

Georgievska, B., Kirik, D., and Bjorklund, A. (2002). Aberrant sprouting and downregulation of tyrosine hydroxylase in lesioned nigrostriatal dopamine neurons induced by long-lasting overexpression of glial cell line derived neurotrophic factor in the striatum by lentiviral gene transfer. Exp. Neurol. 177, 461–474.

Georgievska, B., Kirik, D., and Bjorklund, A. (2004). Overexpression of glial cell line-derived neurotrophic factor using a lentiviral vector induces time- and dose-dependent downregulation of tyrosine hydroxylase in the intact nigrostriatal dopamine system. J. Neurosci. 24, 6437–6445.

Gill, S.S., Patel, N.K., Hotton, G.R., O'Sullivan, K., McCarter, R., Bunnage, M., Brooks, D.J., Svendsen, C.N., and Heywood, P. (2003). Direct brain infusion of glial cell line-derived neurotrophic factor in Parkinson disease. Nat. Med. 9, 589–595.

Hadaczek, P., Kohutnicka, M., Krauze, M.T., Bringas, J., Pivirotto, P., Cunningham, J., and Bankiewicz, K. (2006a). Convection-enhanced delivery of adeno-associated virus type 2 (AAV2) into the striatum and transport of AAV2 within monkey brain. Hum. Gene Ther. 17, 291–302.

Hadaczek, P., Yamashita, Y., Mirek, H., Tamas, L., Bohn, M.C., Noble, C., Park, J.W., and Bankiewicz, K. (2006b). The "perivascular pump" driven by arterial pulsation is a powerful mechanism for the distribution of therapeutic molecules within the brain. Mol. Ther. 14, 69–78.

Hoffman, D., Wahlberg, L., and Aebischer, P. (1990). NGF released from a polymer matrix prevents loss of ChAT expression in basal forebrain neurons following a fimbria–fornix lesion. Exp. Neurol. 110, 39–44.

Holm, P.C., Akerud, P., Wagner, J., and Arenas, E. (2002). Neurturin is a neuritogenic but not a survival factor for developing and adult central noradrenergic neurons. J. Neurochem. 81, 1318–1327.

Johnston, L.C., Su, X., Maguire-Zeiss, K., Horovitz, K., Ankoudinova, I., Guschin, D., Hadaczek, P., Federoff, H.J., Bank-

iewicz, K., and Forsayeth, J. (2008). Human interleukin-10 gene transfer is protective in a rat model of Parkinson's disease. Mol. Ther. 16, 1392–1399.

Kanter-Schlifke, I., Georgievska, B., Kirik, D., and Kokaia, M. (2007). Brain area, age and viral vector-specific glial cell-line-derived neurotrophic factor expression and transport in rat. Neuroreport 18, 845–850.

Kish, S.J., Robitaille, Y., El-Awar, M., Clark, B., Schut, L., Ball, M.J., Young, L.T., Currier, R., and Shannak, K. (1992). Striatal monoamine neurotransmitters and metabolites in dominantly inherited olivopontocerebellar atrophy. Neurology 42, 1573–1577.

Kordower, J.H., Emborg, M.E., Bloch, J., Ma, S.Y., Chu, Y., Leventhal, L., McBride, J., Chen, E.Y., Palfi, S., Roitberg, B.Z., Brown, W.D., Holden, J.E., Pyzalski, R., Taylor, M.D., Carvey, P., Ling, Z., Trono, D., Hantraye, P., Deglon, N., and Aebischer, P. (2000). Neurodegeneration prevented by lentiviral vector delivery of GDNF in primate models of Parkinson's disease. Science 290, 767–773.

Kozlowski, D.A., Bremer, E., Redmond, D.E., Jr., George, D., Larson, B., and Bohn, M.C. (2001). Quantitative analysis of transgene protein, mRNA, and vector DNA following injection of an adenoviral vector harboring glial cell line-derived neurotrophic factor (GDNF) into the primate caudate nucleus. Mol. Ther. 3, 256–261.

Krauze, M.T., Vandenberg, S.R., Yamashita, Y., Saito, R., Forsayeth, J., Noble, C., Park, J., and Bankiewicz, K.S. (2008). Safety of real-time convection-enhanced delivery of liposomes to primate brain: A long-term retrospective. Exp. Neurol. 210, 638–644.

Lategan, A.J., Marien, M.R., and Colpaert, F.C. (1992). Suppression of nigrostriatal and mesolimbic dopamine release *in vivo* following noradrenaline depletion by DSP-4: A microdialysis study. Life Sci. 50, 995–999.

Love, S., Plaha, P., Patel, N.K., Hotton, G.R., Brooks, D.J., and Gill, S.S. (2005). Glial cell line-derived neurotrophic factor induces neuronal sprouting in human brain. Nat. Med. 11, 703–704.

Lowenstein, P.R., and Castro, M.G. (2003). Inflammation and adaptive immune responses to adenoviral vectors injected into the brain: Peculiarities, mechanisms, and consequences. Gene Ther. 10, 946–954.

Lowry, O.H., Rosebrough, N.J., Farr, A.L., and Randall, R.J. (1951). Protein measurement with the Folin phenol reagent. J. Biol. Chem. 193, 265–275.

Maswood, N., Grondin, R., Zhang, Z., Stanford, J.A., Surgener, S.P., Gash, D.M., and Gerhardt, G.A. (2002). Effects of chronic intraputamenal infusion of glial cell line-derived neurotrophic factor (GDNF) in aged rhesus monkeys. Neurobiol. Aging 23, 881–889.

Matsushita, T., Elliger, S., Elliger, C., Podsakoff, G., Villarreal, L., Kurtzman, G.J., Iwaki, Y., and Colosi, P. (1998). Adeno-associated virus vectors can be efficiently produced without helper virus. Gene Ther. 5, 938–945.

McCormack, A.L., Di Monte, D.A., Delfani, K., Irwin, I., Delanney, L.E., Langston, W.J., and Janson, A.M. (2004). Aging of the nigrostriatal system in the squirrel monkey. J. Comp. Neurol. 471, 387–395.

Morgan, J.I., and Curran, T. (1986). Role of ion flux in the control of c-*fos* expression. Nature 322, 552–555.

Munoz, A., Lopez-Real, A., Labandeira-Garcia, J.L., and Guerra, M.J. (2003). Interaction between the noradrenergic and serotonergic systems in locomotor hyperactivity and striatal expression of Fos induced by amphetamine in rats. Exp. Brain Res. 153, 92–99.

Nyholm, D. (2007). The rationale for continuous dopaminergic stimulation in advanced Parkinson's disease. Parkinsonism Relat. Disord. 13(Suppl.), S13–S17.

Pakkenberg, H., Andersen, B.B., Burns, R.S., and Pakkenberg, B. (1995). A stereological study of substantia nigra in young and old rhesus monkeys. Brain Res. 693, 201–206.

Palfi, S., Leventhal, L., Chu, Y., Ma, S.Y., Emborg, M., Bakay, R., Deglon, N., Hantraye, P., Aebischer, P., and Kordower, J.H. (2002). Lentivirally delivered glial cell line-derived neurotrophic factor increases the number of striatal dopaminergic neurons in primate models of nigrostriatal degeneration. J. Neurosci. 22, 4942–4954.

Papailiou, A., Sullivan, E., and Cameron, J.L. (2008). Behaviors in rhesus monkeys (*Macaca mulatta*) associated with activity counts measured by accelerometer. Am. J. Primatol. 70, 185–190.

Parent, A., Charara, A., and Pinault, D. (1995). Single striatofugal axons arborizing in both pallidal segments and in the substantia nigra in primates. Brain Res. 698, 280–284.

Patel, N.K., Bunnage, M., Plaha, P., Svendsen, C.N., Heywood, P., and Gill, S.S. (2005). Intraputamenal infusion of glial cell line-derived neurotrophic factor in PD: A two-year outcome study. Ann. Neurol. 57, 298–302.

Rommelfanger, K.S., and Weinshenker, D. (2007). Norepinephrine: The redheaded stepchild of Parkinson's disease. Biochem. Pharmacol. 74, 177–190.

Rommelfanger, K.S., Edwards, G.L., Freeman, K.G., Liles, L.C., Miller, G.W., and Weinshenker, D. (2007). Norepinephrine loss produces more profound motor deficits than MPTP treatment in mice. Proc. Natl. Acad. Sci. U.S.A. 104, 13804–13809.

Rosenblad, C., Georgievska, B., and Kirik, D. (2003). Long-term striatal overexpression of GDNF selectively downregulates tyrosine hydroxylase in the intact nigrostriatal dopamine system. Eur. J. Neurosci. 17, 260–270.

Sanchez, H.L., Silva, L.B., Portiansky, E.L., Herenu, C.B., Goya, R.G., and Zuccolilli, G.O. (2008). dopaminergic mesencephalic systems and behavioral performance in very old rats. Neuroscience 154, 1598–1606.

Sanftner, L.M., Suzuki, B.M., Doroudchi, M.M., Feng, L., McClelland, A., Forsayeth, J.R., and Cunningham, J. (2004). Striatal delivery of rAAV-hAADC to rats with preexisting immunity to AAV. Mol. Ther. 9, 403–409.

Sarabi, A., Hoffer, B.J., Olson, L., and Morales, M. (2003). Glial cell line neurotrophic factor-family receptor α-1 is present in central neurons with distinct phenotypes. Neuroscience 116, 261–273.

Sherer, T.B., Fiske, B.K., Svendsen, C.N., Lang, A.E., and Langston, J.W. (2006). Crossroads in GDNF therapy for Parkinson's disease. Mov. Disord. 21, 136–141.

Slevin, J.T., Gerhardt, G.A., Smith, C.D., Gash, D.M., Kryscio, R., and Young, B. (2005). Research on Parkinson disease. J. Neurosurg. 102, 401.

Slevin, J.T., Gash, D.M., Smith, C.D., Gerhardt, G.A., Kryscio, R., Chebrolu, H., Walton, A., Wagner, R., and Young, A.B. (2006). Unilateral intraputaminal glial cell line-derived neurotrophic factor in patients with Parkinson disease: Response to 1 year each of treatment and withdrawal. Neurosurg. Focus 20, E1.

Suwelack, D., Hurtado-Lorenzo, A., Millan, E., Gonzalez-Nicolini, V., Wawrowsky, K., Lowenstein, P.R., and Castro, M.G. (2004). Neuronal expression of the transcription factor Gli1 using the Tα1 α-tubulin promoter is neuroprotective in an experimental model of Parkinson's disease. Gene Ther. 11, 1742–1752.

Tanner, C.M., and Goldman, S.M. (1996). Epidemiology of Parkinson's disease. Neurol. Clin. 14, 317–335.

Walton, A., Branham, A., Gash, D.M., and Grondin, R. (2006). Automated video analysis of age-related motor deficits in monkeys using EthoVision. Neurobiol. Aging 27, 1477–1483.

Wright, J.F., Qu, G., Tang, C., and Sommer, J.M. (2003). Recombinant adeno-associated virus: formulation challenges and strategies for a gene therapy vector. Curr. Opin. Drug Discov. Devel. 6, 174–178.

Yang, J., Zhou, W., Zhang, Y., Zidon, T., Ritchie, T., and Engelhardt, J.F. (1999). Concatamerization of adeno-associated virus circular genomes occurs through intermolecular recombination. J. Virol. 73, 9468–9477.

Address reprint requests to:
Dr. Krystof Bankiewicz
Department of Neurological Surgery
1855 Folsom Street, MCB 226
University of California San Francisco
San Francisco, CA 94103-0555

E-mail: Krystof.Bankiewicz@ucsf.edu